Wetlands Ecol Manage
DOI 10.1007/s11273-014-9359-1

ORIGINAL PAPER

Combining ALOS/PALSAR derived vegetation structure and inundation patterns to characterize major vegetation types in the Mamirauá Sustainable Development Reserve, Central Amazon floodplain, Brazil

Jefferson Ferreira-Ferreira · Thiago Sanna Freire Silva · Annia Susin Streher · Adriana Gomes Affonso · Luiz Felipe de Almeida Furtado · Bruce Rider Forsberg · João Valsecchi · Helder Lima Queiroz · Evlyn Márcia Leão de Moraes Novo

Received: 2 November 2013 / Accepted: 24 May 2014

Abstract Remote sensing studies of vegetation cover and hydrologic dynamics in Amazonian wetlands have been mostly limited temporally or spatially, and the distribution and spatial configuration of Amazonian várzea habitats remains poorly known. This study uses multitemporal PALSAR L-band radar imagery combined with object-based image analysis, data mining techniques and field data to derive vegetation structure and inundation patterns and characterize major vegetation types in várzea forests of the Mamirauá Sustainable Development Reserve. Our results show that the combination of vegetation cover and inundation extent information can be a good indicator of the complex gradient of habitats along the floodplain. The intersection between vegetation and flood duration classes showed a wider range of combinations than suggested from field based studies. *Chavascal* areas—chacaracterized as a dense and species-poor shrub/tree community developing in old depressions, abandoned channels, and shallow lakes—had shorter inundation periods than the usually recognized hydroperiod of 180–240 days of flooding, while low várzea—a diverse community that have fewest and smallest species, and highest individual density and that tolerate 120–180 days of flooding every year—was distributed between flood duration ranges that were higher than reported by the literature. Forest communities growing at sites that were never mapped as flooded could indicate areas that only flood during extreme hydrological events, for short periods of time. Our results emphasize the potential contribution of SAR remote sensing to the monitoring and management of wetland environments, providing not only accurate information on spatial landscape configuration and vegetation distribution, but also

Electronic supplementary material The online version of this article (doi:10.1007/s11273-014-9359-1) contains supplementary material, which is available to authorized users.

J. Ferreira-Ferreira (✉) · A. S. Streher · J. Valsecchi · H. L. Queiroz
Instituto de Desenvolvimento Sustentável Mamirauá, Estrada do Bexiga, 2584, Bairro Fonte Boa, Tefé, AM 69470-000, Brazil
e-mail: jefferson.ferreira@mamiraua.org.br

T. S. F. Silva
Departamento de Geografia, Instituto de Geociências e Ciências Exatas de Rio Claro, UNESP - Universidade Estadual Paulista Júlio de Mesquita Filho, Avenida 24-A, 1515 - Jardim Bela Vista, Rio Claro, SP 13506-900, Brazil

A. G. Affonso · L. F. de Almeida Furtado · E. M. L. M. Novo
Divisão de Sensoriamento Remoto, Coordenação Geral de Observação da Terra, Instituto Nacional de Pesquisas Espaciais, Avenida dos Astrounautas, 1758, Caixa Postal, 515 - Jardim da Granja, São José dos Campos, SP 12200-243, Brazil

B. R. Forsberg
Coordenação de Dinâmica Ambiental, Instituto Nacional de Pesquisas da Amazônia, Avenida André Araújo, 2936 – Aleixo, Manaus, AM 69060-000, Brazil

Published online: 11 June 2014

important insights on the ecohydrological processes that ultimately determine the distribution of complex floodplain habitat mosaics.

Keywords Wetlands · Amazonian várzeas · Synthetic aperture radar · Object-oriented image analysis · Random forests · Management · Conservation

Introduction

The Amazonian várzea comprises the floodplains influenced by the sediment-rich white-water rivers of the Amazon basin (Sioli 1954; Prance 1979; Junk et al. 2012). These environments cover an area of about 400,000 km^2, or nearly 12 % of all wetlands in the basin, contributing significantly to the regional carbon balance and biodiversity (Melack et al. 2009; Melack and Hess 2010; Junk et al. 2011). The Solimões/Amazon River várzeas are characterized by an annual flood regime described as the "flood pulse" (Junk et al. 1989). Average maximum flooding depths can reach up to 16 m in Western Amazonia, 10 m in Central Amazonia, and 6 m in Eastern Amazonia, and local flooding extent and duration depends on the interaction between precipitation, river discharge and topography (Junk 1989; Lesack and Melack 1995; Bonnet et al. 2008; Ramalho et al. 2009).

The flood pulse is the main ecological forcing in the floodplain, controlling the occurrence and distribution of plants and animals, life-history traits, primary and secondary production, and also influencing carbon respiration, decomposition and nutrient cycles in water and soils (Junk 1997). Together with geomorphological characteristics, the flood pulse is also directly related to erosion, transport and deposition processes (Irion et al. 1997). Most floodplain environments have a flooding gradient from aquatic to terrestrial conditions, resulting in a complex mosaic of habitats (Junk 1997). Hydrogeomorphological dynamics such as migrating channels and evolving lakes are also an important feature of the várzea landscape, influencing habitat characteristics and vegetation distribution (Wittmann et al. 2004; Peixoto et al. 2009).

Ducke and Black (1953), Rodrigues (1961) and Takeuchi (1962) identified different habitat types, flooding regimes, nutrient availability and biogeographical history as factors influencing the composition, distribution, and diversity of species. Prance (1979) offered the first classification of Amazonian wetland forests, based on hydrological and hydrochemical parameters, and Pires and Koury (1959) and Hueck (1966) described a zonation of plant communities along the flooding gradient in eastern and central Amazonian várzeas. Plants subject to waterlogging have a variety of evolutionary adaptation strategies for coping with the anaerobic soil conditions, and flooding is considered to be the major driver of local-scale habitat zonation, a selective force influencing evolutionary processes (Wittmann et al. 2010b; Parolin et al. 2010).

Junk (1989) reported associations between tree species and topographic heights, with inundations lasting 140 or less days per year, 140–230 days per year, and 230–270 days per year. Applying the nomenclature used by the local population, Ayres (1993) described different várzea forest types according to the mean inundation depth along the lower Japurá River. He described the *chavascal* as a vegetation community of dense shrubs with small trees occurring in areas where the water column depth ranged between 5 and 7 m; the low *restinga* as the vegetation community of forest occupying low land where the seasonal maximum inundation depth ranged between 2.5 and 5 m; high *restinga* as the vegetation community of forest occupying higher land where water column depth ranged from 1 to 2.5 m. Wittmann et al. (2002) updated this classification, modifying the terminology to *várzea alta* (high várzea) and *várzea baixa* (low várzea), to avoid confusion with the term *restinga* as used for coastal vegetation in the Brazilian literature (Fig 1). Recently, Junk et al. (2012) have proposed a comprehensive classification of várzea habitats, based on a combination of hydrological, geomorphological and botanical characteristics. However, given the large extent and heterogeneity of várzea landscapes, little is currently known about the distribution, extent and relative proportion of each of these habitats within the Amazon Basin.

Remote sensing methods have been successfully used to study vegetation cover and hydrologic dynamics in wetland environments, and recent advances have allowed the characterization and quantification of multiple wetland ecological processes (Ozesmi and Bauer 2002; Costa et al. 2013). A few contributions to the understanding of ecological and anthropogenic

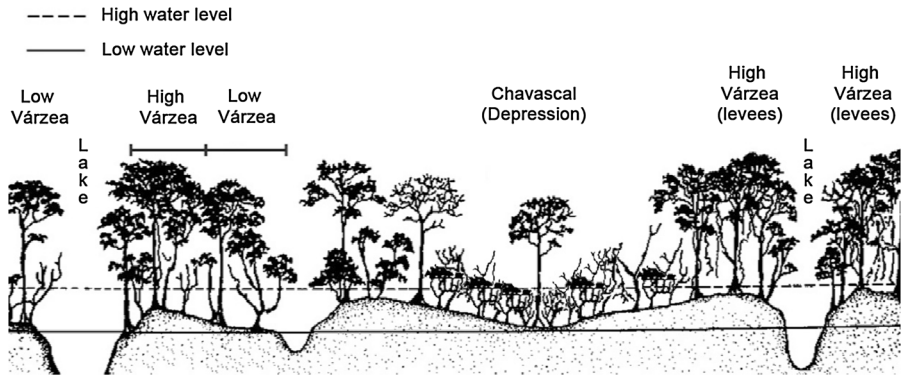

Fig. 1 Conceptual cross-section diagram showing the three main forest types present in Mamirauá Sustainable Development Reserve (Central Amazon, Brazil). Adapted from Ayres (1993)

processes in várzea habitats have been derived from optical remote sensing studies (Mertes et al. 1995; Wittmann et al. 2002; Renó et al. 2011), but most advances have been based on the use of synthetic aperture radar (SAR) sensors, given their ability to detect flooding under plant canopies, and its capacity to acquire images even under cloudy conditions (Kasischke 1997; Henderson and Lewis 2008). Early SAR studies in the floodplain were supported by the SIR-C/X-SAR mission (Hess et al. 1995), and the launch of the Japanese JERS-1 L-band orbital sensor fostered studies on flooding dynamics, habitat mapping, water level height, and biomass estimation (Alsdorf et al. 2007; Rosenqvist et al. 2002; Martinez and LeToan 2007; Costa 2004, 2005; Hess et al. 2003; Hamilton et al. 2007; Forsberg et al. 2001). More recently, the combination of new processing methods such as object-based image analysis (OBIA) and imagery provided by the new crop of polarimetric SAR systems (ALOS/PALSAR, Radarsat-2, TerraSAR-X and Cosmo/Skymed) has allowed researchers to assess vegetation properties and ecological processes in the Amazon floodplain at the landscape scale (Silva et al. 2013; Hawes et al. 2012; Sartori et al. 2011; Arnesen et al. 2013).

Still, most of these studies are limited either temporally or spatially, and the distribution and spatial configuration of várzea habitats remains poorly known, limiting management, monitoring, and conservation initiatives and leaving these areas open to anthropogenic degradation and overexploitation. In this sense, remote sensing monitoring may not only offer a valuable scientific tool, but also contribute directly to the identification of priority areas for protection and conservation, as well as contributing to the proper management of these areas. For this reason, the present study demonstrates how L-band ALOS/PALSAR imagery can be utilized to (1) identify the distribution and relative proportion of different vegetation types, and (2) produce landscape-scale estimates of flooding extent and duration, within the context of management and conservation needs of the Mamirauá Sustainable Development Reserve protected area, in the Central Amazon floodplain.

Methods

Study area

First of its kind, the Mamirauá Sustainable Development Reserve (MSDR) is located on a floodplain region at the confluence of the Solimões (Amazon) and Japurá Rivers, near the town of Tefé and approximately 600 km upstream from the city of Manaus, in the Central Amazon floodplain (Fig. 2). Covering approximately 11,240 km^2, the MSDR is the largest Brazilian protected area dedicated to wetland environmental conservation, and one of the few functional protected areas in the Brazilian várzea forests (Queiroz and Peralta 2006). Recognized as a World Heritage site by UNESCO (http://whc.unesco.org/en/list/998), the MSDR is also currently the only RAMSAR site representing Amazon wetlands (Ramsar Convention Secretariat 2013). Since 1992, active research programs and community-based management projects have been developed in the reserve to understand the biology and conservation of IUCN listed species, such as the Amazonian manatee (*Trichechus inunguis*—vulnerable), the jaguar (*Panthera onca*—near threatened), the Black Caiman (*Melanosuchus niger*—lower risk/conservation

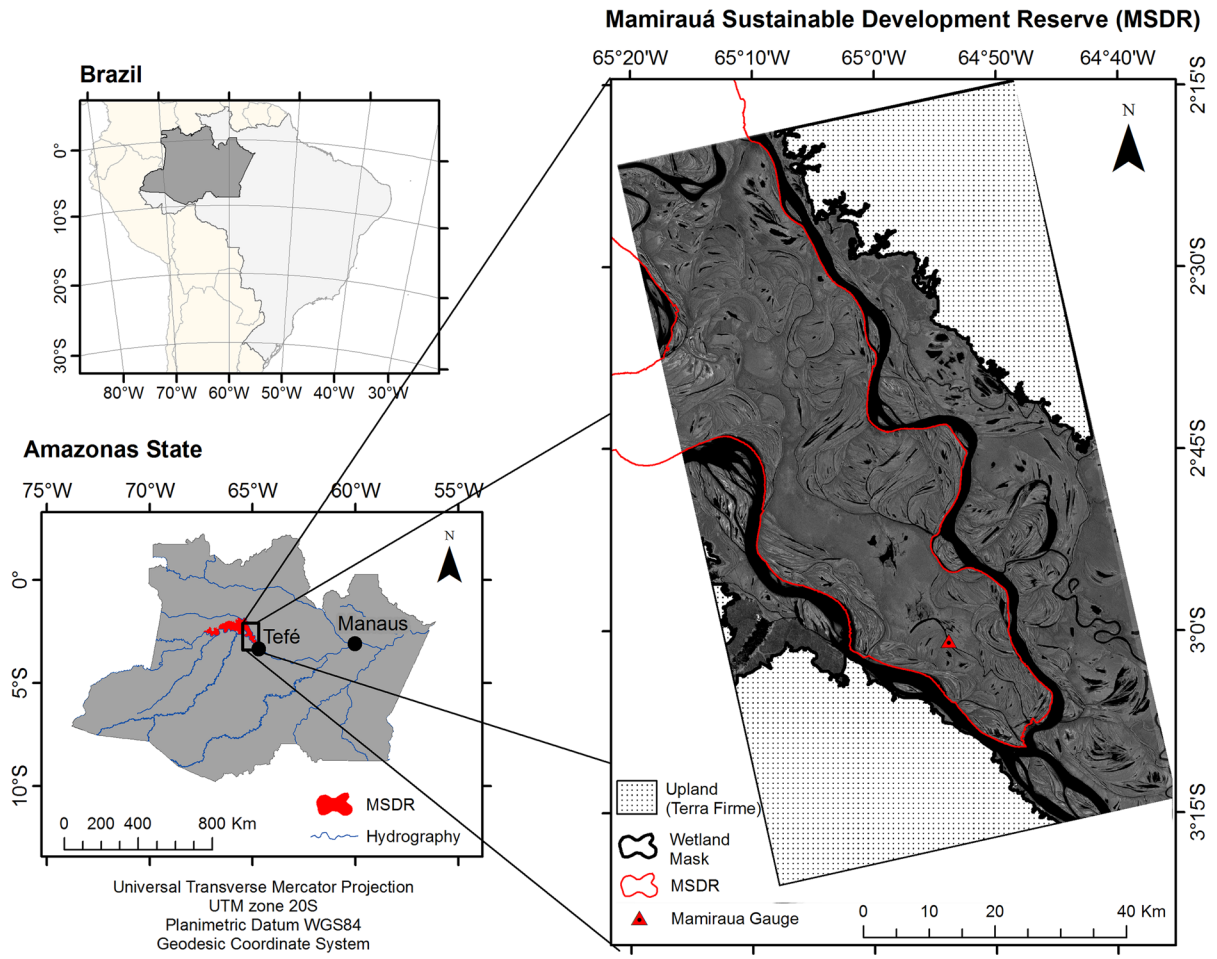

Fig. 2 Mamirauá Sustainable Development Reserve (MSDR) location, in the Central Amazon floodplain, Brazil. On the right, the focal research area of MSDR, located between the Solimões (Amazon) and Japurá rivers, and its adjacent wetlands. The underlying image is a temporal average from a set of 13 HH ALOS/PALSAR image mosaics. The wetlands mask shown was derived from Hess et al. (2003), geometrically corrected by Rennó et al. (2013) and manually edited by Ferreira et al. (2013). ALOS ScanSAR image © JAXA/METI 2013

dependent), and the white *uakari* monkey (*Cacajao calvus*—vulnerable), while promoting sustainable use and protecting the traditional livelihoods of riverine communities. Supporting a range of socio-economic and biological studies on forestry, agriculture, fisheries and ecotourism, the reserve is a key center for research on sustainable development and conservation in Amazonian environments (Schöngart and Queiroz 2010; Queiroz and Peralta 2006; Sociedade Civíl Mamirauá 1996).

Flooding dynamics at the MSDR are characterized by a large monomodal flood pulse, reaching about 10 m in amplitude (Ramalho et al. 2009). The high water phase (*cheia*) starts in May, extending to mid-July, followed by a receding water phase (*vazante*) that lasts until September. The low water phase (*seca*) occurs from September to November, when the rising water phase (*enchente*) phase starts, lasting from December to May (Ramalho et al. 2009).

The main vegetation types observed in the reserve are the chavascal, low várzea, and high várzea, in addition to herbaceous vegetation stands. The chavascal name is given to poorly drained alluvial relicts developing in old depressions, abandoned channels, and shallow lakes, filled with large proportions of clay deposited during the aquatic phase and covered by a dense and species-poor shrub/tree community (Wittmann et al. 2010b). The flood duration in these habitats

is reported as lasting about 180–240 days per year, with water heights varying between 5 and 7 m. Individual density may exceed 600 individuals ha^{-1}, with characteristic species such as *Symmeria* spp., *Calyptranthes multiflora*, *Eugenia ochrophloea*, *Buchenavia oxycarpa* and *Pseudobombax munguba* (Wittmann et al. 2010b).

Low and high várzea habitats are differentiated by floristic and structural features induced by the hydroperiod, sharing between them only ~12 % of the tree species (Wittmann et al. 2002). Due to the stronger flooding pressure, low várzea areas have the fewest and smallest species, and higher individual density. Early successional stages are usually formed by dense and often monospecific stands of *Cecropia latiloba*, which decrease hydrodynamic energy, induce sedimentation, and provide the necessary shading to support the establishment of other species (Wittmann et al. 2010a, b). Late-successional stages usually contain 70–90 species per ha, such as *Piranhea trifoliata*, *Tabebuia barbata, Hevea* spp., *Pouteria* spp., *Oxandra* spp. and *Duroia duckei*. These forests tolerate flood durations of 120–180 days every year, with a water level of 2.5–5 m (Wittmann et al. 2010b).

On high várzea communities, population dynamics and canopy architecture are more complex, with higher biomass, species richness and diversity values than low várzea. In a survey conducted by Wittmann et al. (2002) in the focal research area of the MSDR, 177 species were found in a single 1 ha plot, where 101 species were represented by a single individual. These communities occur in the highest elevations, with a geomorphological context of relative stability, such as scrollbars and levees, and have a distinctive vertical stratification, with an upper canopy height of 30–35 m and emergent trees reaching heights of up to 45 m. Some representative species are *Pouteria procera*, *Malouetia tamaquarina, Aspidosperma riedelii, Guatteriopsis paraensis, Gustavia augusta* and *Pseudoxandra polyphleba*. Flood duration varies between 60 and 120 days per year, with maximum depths of 1–2.5 m. Depending on their position along the flooding gradient, some of these forests may experience less than 50 flooding days per year, and not experience any flooding during exceptionally dry years (Schöngart et al. 2004).

In addition to woody vegetation, areas sometimes referred to as várzea fields (*campos de várzea*) are composed of low lying areas and shallow lakes that alternate seasonally between free water surface, exposed sediments and herbaceous vegetation (macrophytes), occupying areas with the longest flooding durations. These communities comprise several aquatic or palustrine grass species (e.g. *Echinochloa polystachya*, *Hymenachne amplexicaulis*, *Paspalum* spp., *Oryza* spp.), as well as floating herbs such as *Eichhornia* spp., *Pistia* spp., *Salvinia* spp., *Ludwigia* spp., *Neptunia* spp., *Nymphoides* spp. and *Victoria amazonica*. Most of these plants have very high growth rates, and can rapidly occupy available substratum, showing significant seasonal and interannual variation in distribution and coverage (Silva et al. 2013).

Remote sensing data and processing

We acquired L-band (23.6 cm wavelength) SAR imagery from the PALSAR sensor onboard the ALOS satellite, operated by the Japanese Aerospace Exploration Agency (JAXA). All images were made available via the ALOS Kyoto & Carbon (K&C) initiative, an international collaboration network established in 2001 by JAXA to address issues on international environmental conventions, carbon cycle science and environmental conservation, providing a systematic global imagery acquisition strategy not found in any other current SAR mission (Rosenqvist et al. 2010).

Images were acquired in two polarization modes: fine beam single (FBS), with HH polarization, and fine beam dual (FBD), with HH and HV polarizations. The Fine Beam mode is characterized by a high resolution strip with a ~70 km swath, a 38.7° of incidence angle (at the scene center) and 12.5 m pixel spacing. (Rosenqvist et al. 2007). To better capture the flood pulse dynamics, a set of 26 scenes (Path 85, Frames 7120 and 7130) were acquired for several dates, chosen to provide the largest and most uniform range of water level conditions within the available imagery for the area. Water stage data was recorded at the Mamirauá Lake gauging station, located in the southern part of the study region (see Fig. 1; Ramalho et al. 2009; IDSM 2013).

For each date, the corresponding adjacent scene pairs were mosaicked to provide complete coverage of the study area, resulting in a final set of 13 images (Table 1). This acquisition pattern encompassed the focal area of the MSDR, forming a seemingly triangular shape upstream of the confluence between

Table 1 ALOS/PALSAR synthetic aperture radar images acquired at different dates and water stage levels, for mapping vegetation types and inundation extent within the Mamirauá Sustainable Development Reserve (Central Amazon, Brazil)

PALSAR fine beam image date	Polarisation mode	Water stage (m)
2007-06-14	FBD	36.06
2007-07-30	FBD	33.37
2007-10-30	FBS	27.00
2007-12-15	FBS	31.07
2008-05-01	FBD	35.12
2008-08-01	FBD	32.85
2008-12-17	FBS	30.02
2009-06-19	FBD	38.32
2010-03-22	FBS	32.72
2010-05-07	FBD	35.65
2010-06-22	FBD	36.28
2010-09-22	FBD	24.71
2010-12-23	FBS	27.38

FBS fine beam single (HH polarized), *FBD* fine beam dual (HH + HV polarized). Stage heights were obtained from the Mamirauá Lake gauging station (Ramalho et al. 2009; IDSM 2013)

the Japurá and Solimões rivers, where most management activities and research studies take place, and also encompassed adjacent wetlands contained within the selected scenes. The total area mapped comprises approximately 4,680 km^2.

All images were acquired at the 1.5 processing level, which includes range and azimuth compression, multilooking, slant to ground range conversion and radiometric and geometric corrections (Japan Space Systems, 2012), and converted to linear backscattering coefficients (σ^0) for statistical summarization. Final results were expressed in dB units, to allow comparisons with the previous literature. For PALSAR Fine Beam products, the conversion to σ^0 follows Eq. 1:

$$\sigma^0 = 10 * \log_{10}(DN^2) - 83 \quad (1)$$

where DN is the backscattering amplitude expressed in digital numbers, and -83 is the calibration coefficient for PALSAR standard products (Shimada et al. 2009).

In addition to PALSAR images, georeferenced multispectral sensor mosaics with 5 m spatial resolution of RapidEye (multiple dates between 2009 and 2011) and 2.5 m spatial resolution of SPOT-5 (acquisition on 2012-11-08) images were utilized as aid for visual interpretation of the land cover classes in the study area. These images were acquired and provided by the Mamirauá Sustainable Development Institute, who manages the MSDR (www.mamiraua.org.br).

Image segmentation and classification

Our study follows a similar approach to Silva et al. (2010) and Arnesen et al. (2013) to map land cover and inundation status in várzea environments, combining multitemporal SAR imagery and OBIA techniques. Standard image classification techniques work solely on a pixel-by-pixel basis, ignoring both the spatial context and the multi-scale information (texture) contained within the image elements, and are overly susceptible to SAR speckle. OBIA methods start by segmenting the image into homogeneous groups of pixels (objects), ideally corresponding to homogeneous land cover features, and allow the use of multiple descriptive statistics and contextual information during the classification process (Blaschke et al. 2010).

Prior to image segmentation, temporal composite images were produced, following Arnesen et al. (2013): temporal average backscattering (TAB), comprising the average backscattering of the entire image series; temporal standard deviation (TSD), comprising the per-pixel standard deviation for all observed values in the series, and lowest water level backscattering (LWB), simply defined as the scene with the lowest observed water stage level (2010-09-22). These seasonal descriptors allow the segmentation and classification to identify groups of pixels with similar time series of Palsar backscatter coefficients. The measures chosen enable vegetation communities to be defined as a combination of vegetation structure and inundation dynamics. These images were filtered using three consecutive passes of a 3 × 3 Gamma filter (Shi and Fung 1994) and converted to an 8-bit radiometric scale, to reduce speckle heterogeneity and increase computational efficiency during segmentation.

The TAB, TSD and LWB images were used as inputs for the multi-resolution segmentation algorithm implemented on eCognition 8.0 (Definiens 2009), together with a vector file of the Amazon wetland mask produced by Hess et al. (2003), geometrically corrected by Rennó et al. (2013) and manually edited

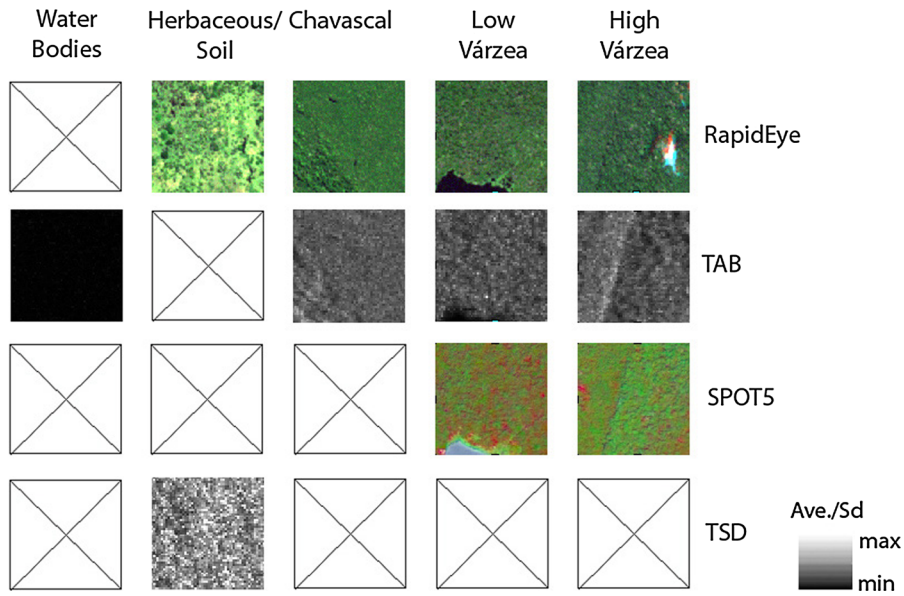

Fig. 3 Visual interpretation key used to select training and validation samples for vegetation mapping at the Mamirauá Sustainable Development Reserve (Central Amazon, Brazil). *TAB* temporal average backscattering, *TSD* temporal standard deviation of backscattering, TAB and TSD were calculated using all available ALOS/PALSAR images of the 2007–2010 time series

by Ferreira et al. (2013). This is a region-merging algorithm that begins with a single pixel and a pairwise comparison with its neighbors, with the goal of minimizing the resulting calculated heterogeneity (Benz 2004). After iterative testing, the parameters of scale = 150, shape = 0.1 and compactness = 0.5 were selected.

After segmentation, the mean and standard deviation of σ^0 were computed for each image object, separately for all 15 available layers (single date images plus TAB and TSD), resulting in a total of 50 object attributes across all dates and polarizations available. For the TAB and TSD seasonal descriptors, the original unfiltered and unscaled images were used to ensure comparability with the single date imagery. Using vegetation type information from 86 survey plots provided by the Mamirauá Institute for Sustainable Development, and supported by Rapid Eye, SPOT-5 and Google Earth™ high resolution imagery, 360 objects were selected as training samples (72 objects per class) for subsequent radiometric analysis and classification, based on a multi-sensor interpretation key (Fig. 3). Five land cover classes recognized in the literature (Ayres 1993; Junk et al. 2012; Wittmann et al. 2002) were defined for evaluation: three main arboreal vegetation types ("Chavascal", "Low Várzea" and "High Várzea"), permanently free water surfaces ("Water Bodies"), and transient areas that alternate seasonally between water, substratum and herbaceous vegetation ("Herbaceous/Soil"). Upland (*terra firme*) areas were excluded using the wetland mask from Hess et al. (2003), and not further evaluated. After sample selection, the temporal radiometric response of each class was graphically analyzed using boxplots.

To discriminate the defined classes, we used the random forests (RF) algorithm, proposed by Breiman (2001), as implemented in the "randomForest" package of the R open source statistical programming environment (Liaw and Wierner 2002). A vector file containing all image objects identified as training samples, with the associated attribute table containing class labels and sampled backscattering responses for all images in the series, was submitted as input to the RF algorithm, to derive the classification tree ensemble. This ensemble was then applied to the entire set of generated image objects, to produce the final classification (see Online Resource 1 for R script).

The RF algorithm is an ensemble learning method based on classification and regression trees (CART, Walker et al. 2010), where instead of a single decision tree, a "forest" (i.e., ensemble) of individual trees is built through randomization of the training data. Final class predictions are based on using a majority voting scheme (consensus) among the trees in the ensemble, improving predictive accuracy. Independent trees are constructed using a bootstrap sample of the data set in a process called "bagging". In each bootstrap sample,

approximately one-third of the reference data are left out. At the end of each iteration, the "out-of-bag" samples are then predicted using the ensemble derived from the bootstrap sample, and later aggregated to produce an out-of-bag (OOB) estimate of classification error for the entire "forest". The two main parameters of the classifier are the number of independent trees generated (n_{tree}) and the number of predictive variables that are randomly selected for choosing the best split (m_{try}). Multiple combinations of the two main parameters were tested until an optimal set of parameters was found.

The accuracy of the vegetation map was assessed using 142 validation points, randomly distributed within the study area using a Geographic Information System software. These points were manually classified based on the predefined interpretation key (Fig. 3), using available high-resolution imagery. The resulting manual classification was compared to the RF classification to build a confusion matrix and derive overall accuracy, class accuracy, kappa statistics (Congalton 1991) and quantity and allocation disagreement measures (Pontius and Millones 2011). Quantity disagreement refers to the difference in area proportions between the reference data (training samples derived from field plots) and the classification. Allocation disagreement, on the other hand, is the proportion of misplaced objects from the classified map in comparison with positions in the reference data. A comparison between a reference map with two classes and a classification where every point is misclassified as the opposite class, for instance, would have 0 % quantity disagreement and 100 % allocation disagreement. Although Pontius and Millones (2011) condemn the use of the kappa index of agreement, we include it here to allow comparisons with previous literature.

Flood extent mapping

Flood extent maps were generated for all single date images based on the expected increase in SAR signals due to enhanced double-bounce scattering, where the radar beam is specularly reflected by the free water surface under the canopy, and then scattered back to the sensor by the standing vegetation, or vice versa (Hess et al. 1995; Silva et al. 2008). Flooded area for woody vegetation was determined based on simple thresholds, determined by the graphical analysis of backscattering values in each PALSAR scene.

Table 2 Water stage for each map of inundation extent, and corresponding flood duration classes, in days, for the Mamirauá Sustainable Development Reserve (Central Amazon, Brazil)

Water stage level (m.a.s.l.)	Flood duration (days)
27.00	>295
30.72	175–295
31.07	175–295
32.72	125–175
33.73	105–125
35.12	40–105
35.65	<40
36.06	<40
38.32	<40

Maps obtained from similar stage levels were combined into a single flood duration class

Once flooded area was determined for each image in the time series, each flood map was associated to a corresponding water level, according to Table 2. Water levels considered too similar in terms of flood extent were grouped into a single class, and the image acquired on 2010-09-22 was excluded from the analysis, since it had a very low water level and negligible flood extent outside of permanent water bodies. This resulted in nine different inundation extent maps, corresponding to each water level (27.0, 30.72, 31.07, 32.72, 33.73, 35.12, 35.65, 36.06 and 38.32 m).

Average flood duration was estimated by taking the average stage height for all available data from the Mamirauá gauge (1991–2011; meters above sea level), and determining the number of days per year where this average was equal or above the observed stage height at the moment of image acquisition. Flood duration categories were then established by taking this duration and extending it backwards until the previously observed duration category (see example on Fig. 4). Stage heights with very similar flood durations were again grouped into the same category, resulting in six flood duration classes. The single final map was derived by successively overlaying inundation maps of consecutive stage heights, and labelling all pairwise non-overlapping mapped areas as flooded between the levels observed for the first and second maps. Finally, all mapped Herbaceous/Soil areas were

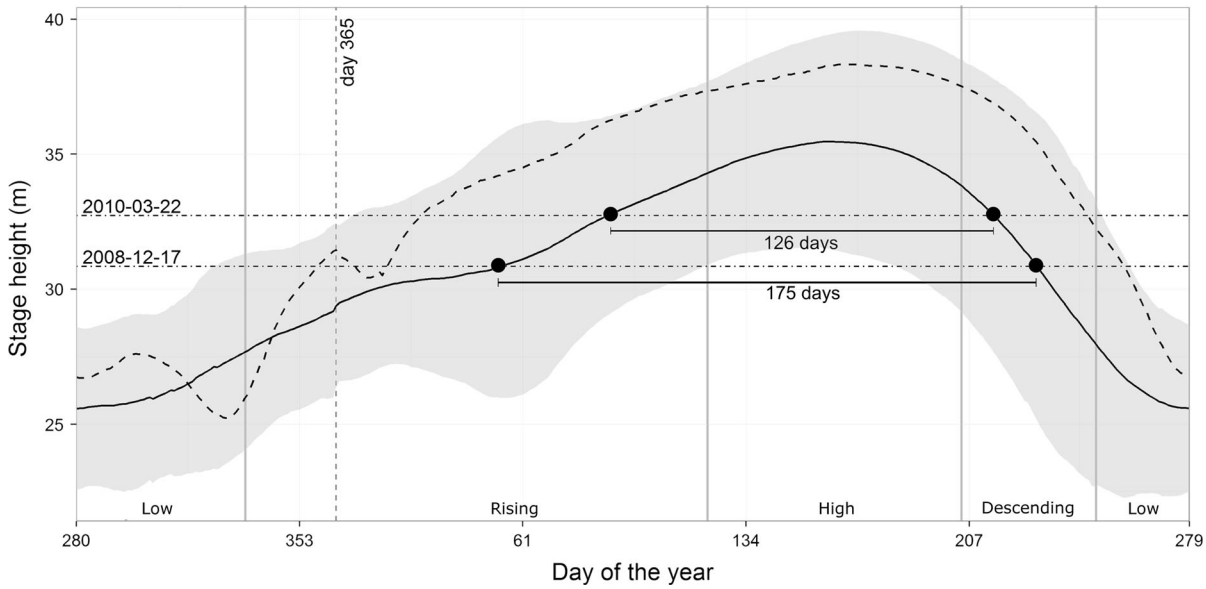

Fig. 4 Mean water stage and shaded 95 % confidence interval for the 1991–2011 period, measured at the Mamirauá Lake gauge, Mamirauá Sustainable Development Reserve (Central Amazon, Brazil) (Ramalho et al. 2009; IDSM 2013). The ordering of the Julian dates is offset, starting at the lowest mean water level to indicate the average onset date for the rising water period. The four stages of the flood pulse are indicated as low, rising, high and descending. The *dashed line* indicates the abnormally high water levels for the 2008–2009 hydrological year, when *iButton* inundation data was recorded (Affonso et al. 2011; Hess et al. 2011). *Horizontal lines* show the stage levels for two hydrologically consecutive image acquisition dates. According to our criteria, flood duration for the 2010-03-22 image is assumed to be between 175 and 125 days

added to the map as belonging to the ">295 flooding days" class, and the mapped Water Bodies class was appended as a "365 flooding days" class.

Flood mapping validation was performed using temperature-based inundation data from Affonso et al. (2011) and Hess et al. (2011), based on thermistor chains (Thermocron® iButtons®). These authors have recovered inundation data from 18 sites within the focal research area of the MSDR, for the 2008–2009 hydrological year. The location of each site was identified on the flood duration map, and the in situ duration of inundation was then compared to the estimated duration derived from the PALSAR time series.

Once both maps were validated, the co-occurrence of vegetation and inundation classes was determined by an overlay of both maps, quantifying the total area for each combination of vegetation type and flood duration.

Results

The best parameterization of the RF algorithm consisted of an ensemble of $n_{tree} = 5000$ decision trees, with $m_{try} = 20$ out of the 50 available predictor variables as candidates for a split. This resulted in an overall estimated OOB error of 10.6 %. The highest prediction errors were observed for Chavascal, with a 20 % prediction error composed mainly of misclassification with low várzea (12.5 %) and high várzea (5.5 %), and for low várzea with 13 % prediction error, equally distributed between Chavascal and high várzea. The remaining classes had prediction errors of 8 % (Herbaceous/Soil), 6 % (high várzea) and 2 % (water bodies).

The resulting classification revealed a dominance of low várzea environments, and an overall complex mosaic of habitats resulting from the dynamic hydrogeomorphological characteristics of the area (Fig. 5). Vegetative cover was distributed as 1,753 km^2 (37.7 %) of low várzea, 873 km^2 (18.7 %) of high várzea, 832 km^2 (18 %) of Chavascal, 711 km^2 (15.3 %) of Water Bodies, and 480 km^2 (10.3 %) of herbaceous/soil. Independent validation of the vegetation cover classification based on comparison with high-resolution optical imagery yielded an overall accuracy of 83 %, with a kappa index of

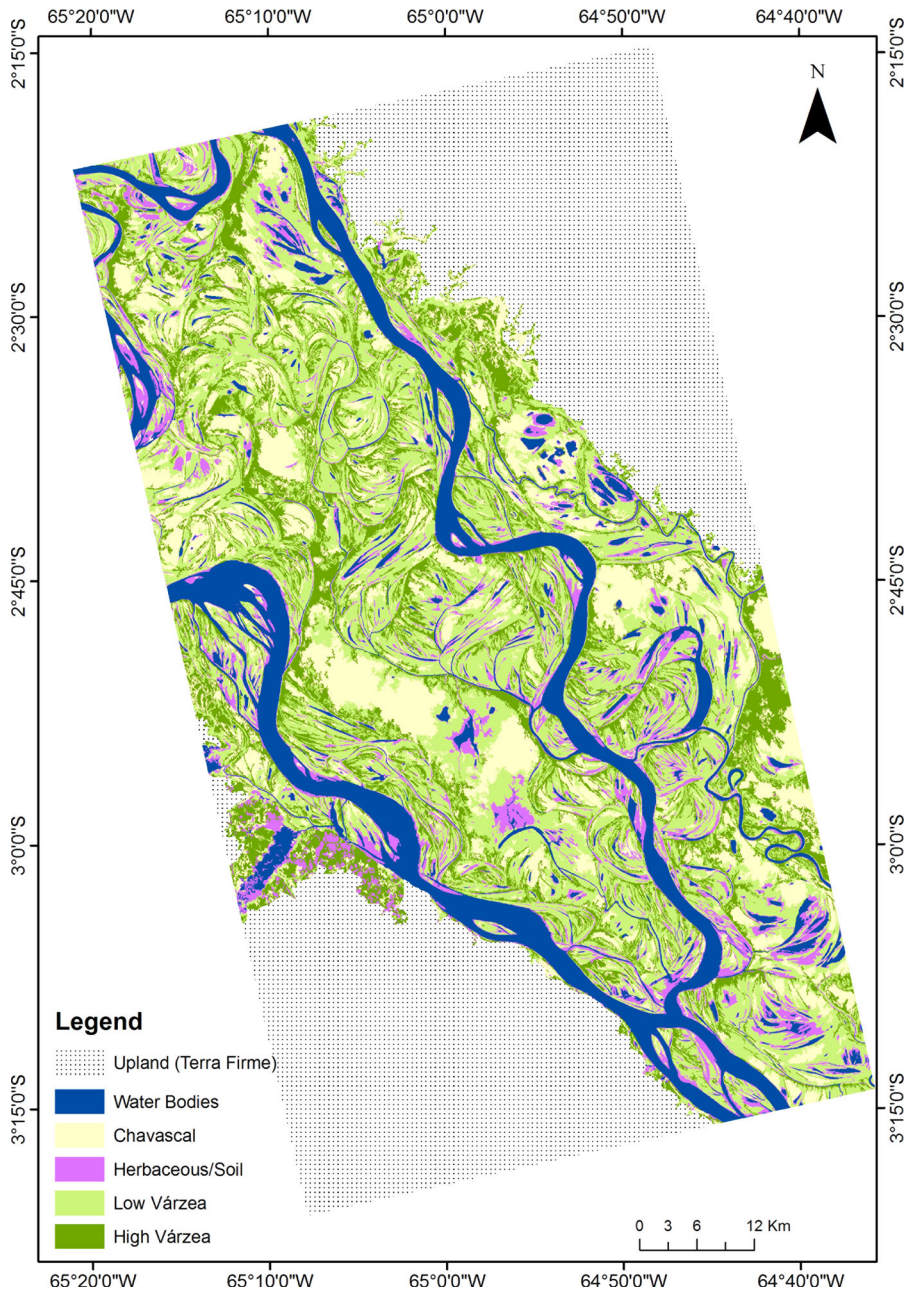

Fig. 5 Major vegetation types and habitats of the focal research area of the Mamirauá Sustainable Development Reserve (Central Amazon, Brazil) and its surroundings, mapped using ALOS/PALSAR image time series, and the random forests classification algorithm

agreement of 0.8 (Table 3). The worst results were again observed for the Chavascal and Low Várzea classes, while the Herbaceous/Soil class had the largest spread of misclassification.

Overall disagreement rates were of 5 % for quantity and 10 % for allocation. The highest allocation disagreement was observed for the Low Várzea class, with 9 % of misplaced objects, followed by Chavascal, with 8 % and High Várzea with 4 %. Both Herbaceous/Soil and Water Bodies did not have a significant amount of misplaced objects. Quantity disagreement indicated underestimation of Herbaceous/Soil ($\sim$4 %), resulting from confusion with Water Bodies, with negligible errors for the remaining classes ($\sim$1–2 %).

Graphical analysis of backscattering values showed the effect of flooding on the radar signal, emphasizing the different patterns of radar backscattering evolution

Table 3 Confusion matrix and accuracy indices for the classification of vegetation types using ALOS/PALSAR image time series and the random forests classification algorithm, for the Mamirauá Sustainable Development Reserve (Central Amazon, Brazil)

	Water bodies	Várzea fields	High várzea	Low várzea	Chavascal
Water bodies	24	3	0	0	0
Várzea fields	0	28	0	0	0
High várzea	0	1	21	6	0
Low várzea	0	3	1	18	7
Chavascal	0	0	1	2	27
N	24	35	23	26	34
% Error	0 %	20 %	8.7 %	30.7 %	20.5 %
Overall 83 % accuracy	Kappa: 0.8	Quantity disagreement	5 %	Allocation disagreement	10 %

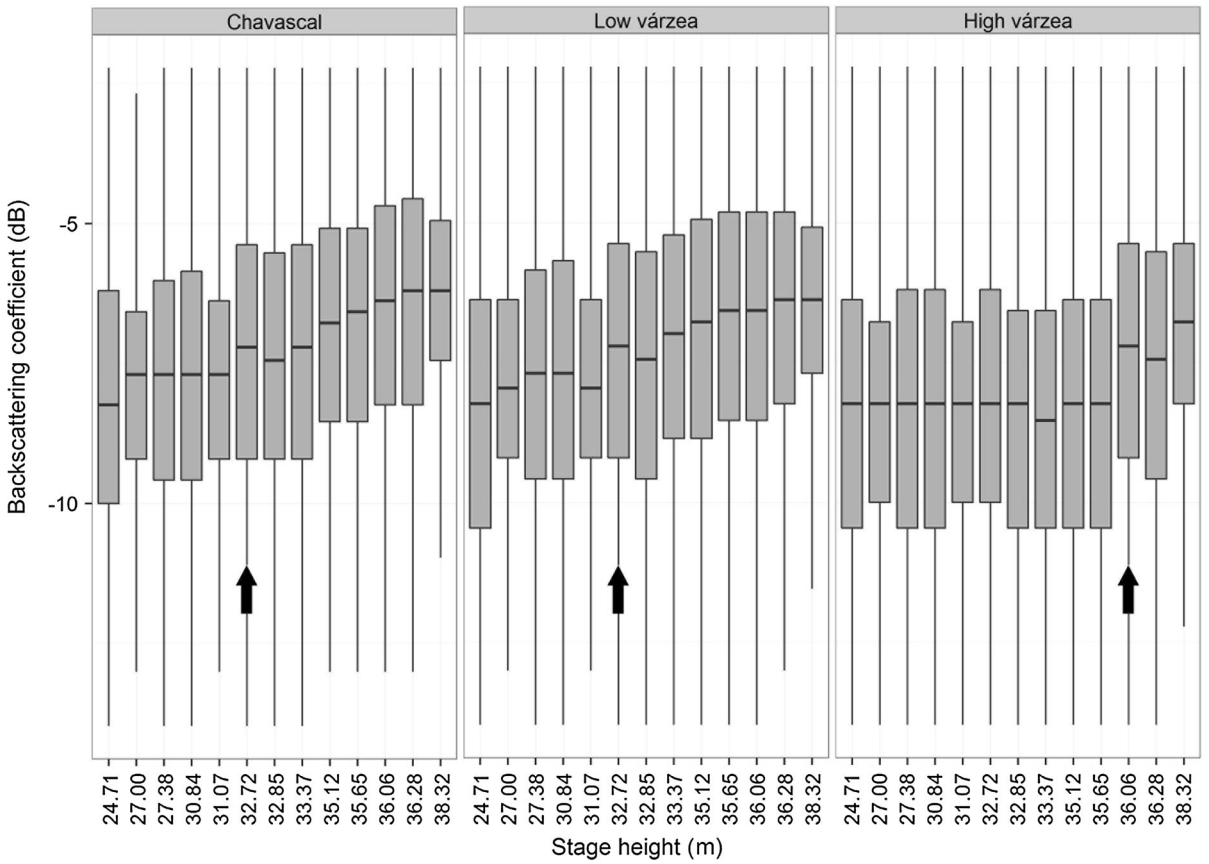

Fig. 6 Temporal variation of ALOS/PALSAR backscattering coefficients for the three main woody vegetation classes occurring on the Mamirauá Sustainable Development Reserve (Central Amazon, Brazil). The *arrows* indicate the period where flooding begins. The different flooding onset and flooding patterns for each class are visible

that reflect different flood regimes for chavascal, low várzea and high várzea environments (Fig. 6). The final image-specific thresholds selected for inundation mapping varied between −6.57 and −5.85 dB, resulting in estimated flooding durations between less than 40 days and more than 295 days, in addition to the permanently flooded areas (Fig. 7, Table 2). Overall, most areas were inundated for less than 40 days or for 125 to 175 days

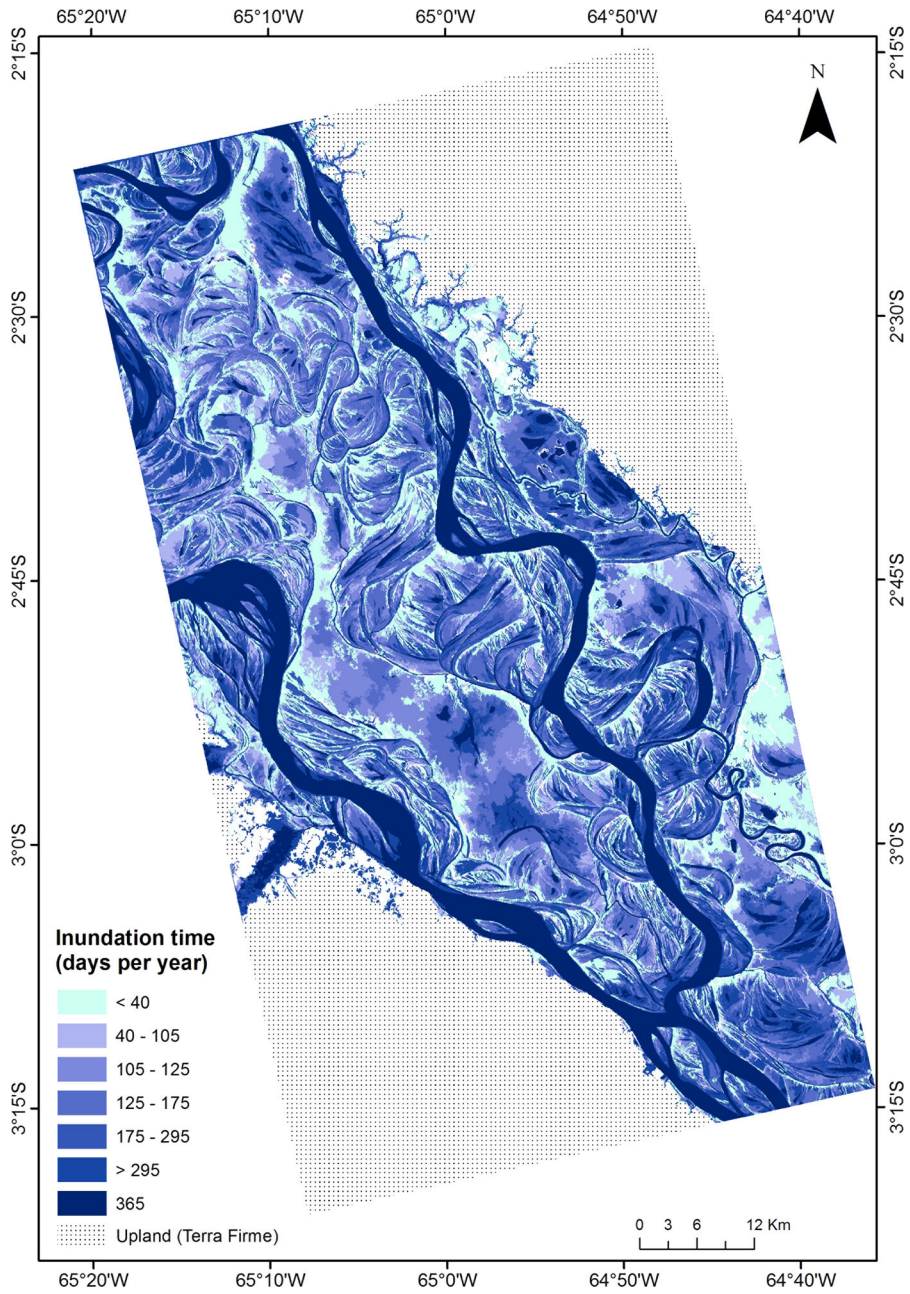

Fig. 7 Estimated duration of inundation, based on a time series of ALOS/PALSAR image data, for the focal research area of the Mamirauá Sustainable Development Reserve and surroundings, Central Amazon floodplain, Brazil

(Fig. 8). The agreement between estimated flood durations and ground data from Affonso et al. (2011) was variable; from the 18 records, eight corresponded to the actual range of estimated flood duration, nine were off by one estimated class, and one was off by two classes (Table 4).

The intersection of vegetation types and flood duration classes showed that chavascal areas had the most varied inundation pattern, covering the entire range of estimated flood duration classes, with a higher frequency (49 %) in the range of 105–125 days of flooding per year (Fig. 9). Low várzea areas, on the other hand, occurred predominantly on the class labeled as 175–295 days of flooding, followed by the 125–175 days of flooding class. High várzea agreed more closely with the expected distribution across the flood duration classes, with the highest frequency being observed at less than 40 days of flooding per

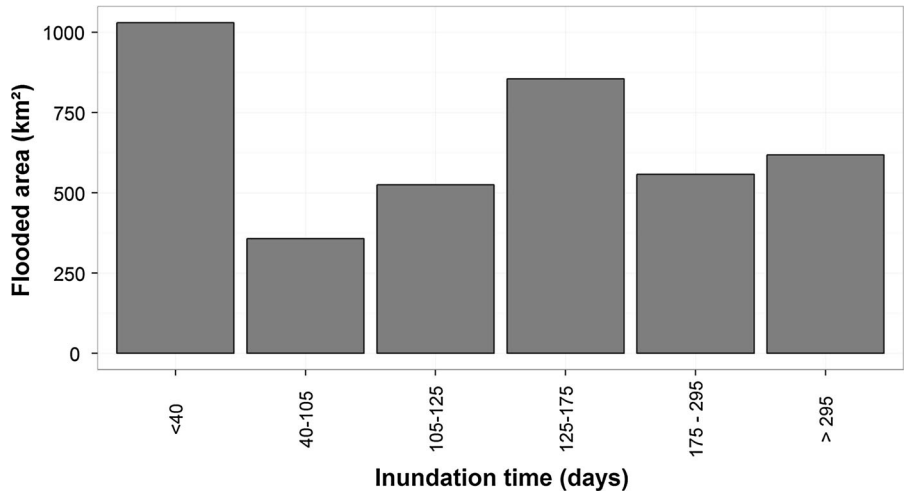

Fig. 8 Extent of estimated flood duration classes (in days), based on ALOS/PALSAR imagery, for the Mamirauá Sustainable Development Reserve (Central Amazon, Brazil)

Table 4 Comparison of flood duration estimates as determined in situ using temperature gauges by Affonso et al. (2011) and Hess et al. (2011) and as derived from ALOS/PALSAR images for the Mamirauá Sustainable Development Reserve (Central Amazon, Brazil)

Station number[a]	Flood duration (days)[a]	Flood duration (days) PALSAR
1	176	125–175
2	233	105–125
3	231	>295
4	217	125–175
5	241	>295
6	291	>295
7	219	175–295
8	237	175–295
9	239	175–295
11	238	175–295
13	240	>295
14	241	125–175
18	239	>295
19	176	175–295
20	238	125–175
21	244	175–295
22	249	>295
23	243	>295

[a] Variables defined in Affonso et al. (2011)

year. Moreover, about 181 km^2 of this class occurred in areas that were never mapped as flooded, considering the existing range of images (and which were added to the "<40 days of flooding class").

Discussion

The RF algorithm was a robust classification technique for várzea vegetation, when coupled with reliable and sufficient ground data and with OBIA methods. The availability of multitemporal information was paramount to obtain accurate class discrimination, as already shown by Martinez and Letoan (2007) and Silva et al. (2010). Due to their higher structural similarity, woody vegetation classes tended to share most of the misclassification errors, which may have led to the overestimation and erroneous allocation of Low Várzea objects, compared to Chavascal and High Várzea. While chavascal areas tend to form more homogenous and densely packed stands and high várzea forests will often correspond to complex, relatively stable vegetation assemblies, low várzea regions can display a wide range of community composition and structural characteristics, depending on relative age and position along the flooding gradient. This variability was translated into well-defined class attributes for High Várzea and Chavascal, while the larger variability of Low Várzea samples increased classification error. L-band SAR data also led to confusion between Herbaceous/soil and water bodies, due the relative similar and smooth surface of these targets at this wavelength. The complementary use of shorter SAR wavelengths, such as C or X bands, could lower this error.

The dynamic geomorphological nature of the study area explains the naturally fragmented landscape mosaic evidenced by our mapping. In this context,

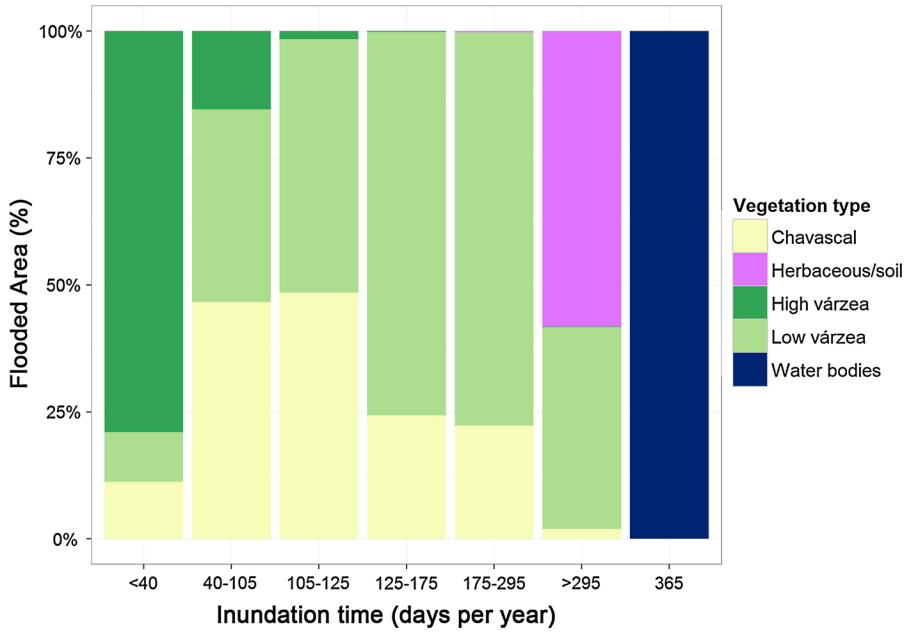

Fig. 9 Relative area for each combination of land cover and flood duration classes derived from ALOS/PALSAR image time series for the Mamirauá Sustainable Development Reserve (Central Amazon, Brazil)

high várzea forests can be seen as the narrowest and most disjoint landscape elements, while chavascal formations tend to form more aggregated, continuous fields. Noteworthy spatial associations were also observed, such as the interrelated distribution of water channels and flood duration, versus chavascal and high várzea distributions. As the chavascal occurs in poorly drained depressions or silted-up lakes, it tends to occupy the backswamps behind the levees covered by high várzea. Eventually, the establishment of pioneer vegetation will increase sediment deposition and raise the terrain level, reducing flood duration and allowing the establishment of other species, in a process of ecological and geomorphological co-evolution (Wittmann et al. 2010b). Given the well-known effect of landscape configuration on the conservation of plant and animal species (Lindenmayer et al. 2008), our detailed vegetation map can enable spatially aware decision making for conservation measures in the MSDR.

Virtually all of the study area was flooded when water levels were close to the peak of the high water phase. Results also showed that 22 % of the evaluated areas were classified as "<40 days of flooding", followed by areas flooded for 125–175 days per year representing about 12 % of the mapped area. The uneven distribution of flooded areas at different water levels results from the stepped nature of the floodplain terrain, where critical water stage heights result in large expansions of inundation area while other heights in the range have minimum effects. The best example of such as process is the water stage height at which transition from channel to overbank flow occurs, immediately inundating the backswamp depressions.

Although the comparison between flood duration and in situ temperature-based observations showed some disagreement, we believe that the maps obtained do represent the overall spatial distribution and variability of flooding in the studied system, and are similar to other products developed for floodplain forest environments in the Amazon (Forsberg et al. 2001; Rosenqvist et al. 2002). Three main sources of error can account for the observed disagreements: positional errors between in situ stations and image data; inherent variability of flood duration, as shown by the confidence intervals on Fig. 3; and the fact that field data was acquired during the 2008–2009 hydrological year, the second largest flood of the last 50 years (Fig. 3), whereas our imagery spans a broader time period. In response to our results, the Mamirauá Sustainable Development Institute is

currently funding the installation of high precision level gauges, tied to surveyed altimetric transects and with accurate geolocation, to properly characterize flooding dynamics in the region. Once such data is available, the current results can be further validated and refined.

The intersection between vegetation and flood duration classes showed a wider range of combinations than expected based on the literature. Chavascal areas had shorter inundation periods than the usually recognized hydroperiod of 180–240 days of flooding (e.g. Ayres 1993; Wittmann et al. 2002), while low várzea was distributed between flood duration ranges that were higher than reported by the literature (120–180 days). This apparent inversion of results is likely owed to the higher misclassification errors between these two classes, implying that forests with a highly variable range of structural and taxonomic characteristics are distributed within the range of approximately 50–200 days of flooding. The graphical analysis of training samples based on actual ground data (Fig. 6) suggests that inundation occurs at similar times for both classes, further adding to the differentiation problem.

While some of the unusual combinations of vegetation and flooding observed likely occurred due to classification errors, these results suggest that such combined information can be a good indicator of the complex gradient of habitats along the floodplain, including the identification of rare habitats. Further verification of these locations in the field could therefore suggest potential areas for special conservation measures, given their relative rarity in the landscape. For example, shrub-like vegetation occurring in areas flooded for short periods (mislabeled as chavascal) could indicate prevailing soil properties, such as high clay content and/or high phreatic levels, while forest communities growing at sites that were never mapped as flooded could indicate areas that only flood during extreme hydrological events, for short periods. As only 31 % of várzea tree species are shared with upland forests, of which 67.5 % are restricted to high várzea (Wittmann et al. 2006), these areas could house species or assemblages that are currently rare in the landscape, but have the potential to become more prevalent under current scenarios of longer dry periods and more frequent extreme climatic events predicted for Amazonian environments (Malhi et al. 2008; Melack and Coe 2013). These areas can therefore have an important conservation role as vegetation refugia for maintaining current and future diversity in the floodplain (Ashcroft et al. 2009).

Management implications

The Amazonian várzeas are endangered ecosystems that require special protection initiatives (Junk et al. 2011). The composition and abundance of various components of the fauna are also associated to várzea environments and its vegetation types (Pereira et al. 2009; Beja et al. 2010; Paim et al. 2013). Detailed knowledge of the distribution and abundance of rare, endemic or threatened species in these environments is needed to define sensitive areas or areas that should be addressed with additional efforts or special protection. The distribution and abundance of different endangered species, such as jaguars (*P. onca*), giant otters (*Pteronura brasiliensis*) and some primates such as the black squirrel monkey (*Saimiri vanzolinii*) or white uacari (*C. calvus*) are also associated with dominant types of forest formation, and the local regime of flooding (Silveira et al. 2010; Lima et al. 2012; Paim et al. 2013).

The flood predictability in the várzea environments is a key factor for a wide range of conservation initiatives and extractive activities of the local population that use the resources of these ecosystems. Large scale predictability already includes flood pulse intensity for some places of the Amazon, such as Manaus and Tefé (Schöngart and Junk 2007), but local scale information on flood dynamics and extent remains unavailable. Such information would allow adequate sustainable use of innumerous natural resources from the várzea ecosystems; for example, access to remote sites within the forest for extractive activities depends on previous information about flood dynamics at these sites. To plan timber exploitation on várzea forests, where there are no roads to transport the logs, local-scale flood predictability is crucial to allow wood transport by rafting during high-water periods (Schöngart and Queiroz 2010). Access to lakes and channels of exceptional productivity for Pirarucu (*Arapaima gigas*) fishing (Viana et al. 2007) and for caiman catching (Botero-Arias et al. 2010), both of which are forms of sustainable resource management in the floodplains at different stages of development, is also related to the predictability of flooding and hydrological dynamics in these locations. Therefore,

providing habitat and flooding maps for the Amazon floodplain can significantly improve the efficiency in developing and managing conservation actions targeted towards these ecosystems.

Conclusions

Our results emphasize the potential contribution of SAR remote sensing to the monitoring and management of wetland environments, providing not only accurate information on spatial landscape configuration and vegetation distribution, but also important insights on the ecohydrological processes that ultimately determine this distribution. SAR systems are unique in their ability to map both vegetation distribution and flooding extent, and the combination of the two, together with a multitemporal approach, offers unique insight into the functioning of wetland ecosystems.

Information derived from the present study also provides a solid basis for the study of plant and animal species distribution and habitat use, as well as an understanding of spatial variability of biogeochemical processes, and may ultimately support ecosystem modeling efforts and the forecasting of different ecological scenarios. It also provides an ideal database for testing the spatial implications of the "flood pulse concept" (Junk et al. 1989), a general theory of floodplain ecosystems which relates flood durations and other hydrological characteristics to the distribution and dynamics of aquatic flora and fauna. We believe our method could be successfully replicated for other seasonal wetland environments, using different kinds of SAR and optical image time series and available open-source remote sensing and statistical software. Given the rising availability of SAR sensors operating at multiple frequencies and spatial configurations, with a plethora of new systems planned or already scheduled for launch in the following years, multitemporal SAR studies could become an affordable and reliable method for wetland ecological monitoring in the Amazon.

Acknowledgments We thank the Instituto Nacional de Pesquisas Espaciais (INPE) for the support during this study, and the Instituto de Desenvolvimento Sustentável Mamirauá (IDSM – OS/MCTI) for the financial support for this research. We also thank João Lanna and Fernanda Paim for sharing the field plot data. Dr. Silva acknowledges postdoctoral funding from the São Paulo Research Foundation (FAPESP grant 2010/11269-2). This work has been undertaken within the framework of JAXA's Kyoto & Carbon Initiative, with ALOS PALSAR data provided by JAXA EORC.

References

Affonso AG, Arraut EM, Renó VF, Leão JAD, Hess, LL, Queiroz HL, Novo EMLM (2011) Estudo da dinâmica de inundação na várzea Amazônica através de termo-sensores de campo. Anais XV Simpósio Brasileiro de Sensoriamento Remoto, pp 5092–5099, ISBN: 978-85-17-00057-7

Alsdorf D, Bates P, Melack J et al (2007) Spatial and temporal complexity of the Amazon flood measured from space. Geophys Res Lett 34:L08402

Arnesen AS, Silva TSF, Hess LL, Novo EMLM, Rudorff CM, Chapman BD, McDonald KC (2013) Monitoring flood extent in the lower Amazon River floodplain using ALOS/PALSAR ScanSAR images. Remote Sens Environ, 130, pp 51–61. http://linkinghub.elsevier.com/retrieve/pii/S0034425712004257. Accessed 30 May 2013

Ashcroft MB, Chisholm LA, French KO (2009) Climate change at the landscape scale: predicting fine-grained spatial heterogeneity in warming and potential refugia for vegetation. Glob Chang Biol 15:656–667

Ayres JM (1993) As matas de várzea do Mamirauá. In: Sociedade Civil Mamirauá (ed) Estudos de Mamirauá. MCT/CNPq, Brasília, pp 1–123

Beja P, Santos CD, Santana J, Pereira MJ, Marques JT, Queiroz HL, Palmeirim JM (2010) Seasonal patterns of spatial variation in understory bird assemblages across a mosaic of flooded and unflooded Amazonian forests. Biodivers Conserv 19(1):129–152

Benz U, Hoffmann P, Willhauck G et al (2004) Multi-resolution, object-oriented fuzzy analysis of remote sensing data for GIS-ready information. ISPRS J Photogramm Remote Sens 58:239–258

Blaschke T (2010) Object based image analysis for remote sensing. ISPRS J Photogramm Remote Sens 65:2–16

Bonnet MP, Barroux G, Martinez JM, Syler F, Moreira-Turcq P, Cochonneau G, Melack JM, Boaventura G, Maurice-Bourgoin L, León JG, Roux JG, Calmante S, Kosuth P, Guyot JL, Seyler P (2008) Floodplain hydrology in na Amazon lake (Lago Grande de Curuaí). J Hydrol 349(1–2):18–30

Botero-Arias R, Marmontel M, Queiroz HL (2010) Projeto de manejo experimental de jacarés no Estado do Amazonas: abate de jacarés no setor Jarauá – Reserva de Desenvolvimento Sustentável Mamirauá, Dezembro de 2008. Uakari 5(2):49–57

Breiman L (2001) Random forests. Mach Learn 45(1):5–32

Congalton R (1991) A review of assessing the accuracy of classifications of remotely sensed data. Remote Sens Environ 37:35–46

Costa MPF (2004) Use of SAR satellites for mapping zonation of vegetation communities in the Amazon floodplain. ISPRS J Photogramm Remote Sens 25(10):1817–1835

Costa MPF (2005) Estimate of net primary productivity of aquatic vegetation of the Amazon floodplain using Radarsat and JERS-1. Int J Remote Sens 26(20):4527–4536

Costa MPF, Silva TSF, Evans TL (2013) Wetland classification. In: Wang G, Weng Q (eds) Remote Sensing of Natural Resources. CRC Press, Boca Raton-FL, pp 461–478

Definiens (2009) Definiens developer 8: User guide. The Imaging Intelligence Company, Munich

Ducke A, Black GA (1953) Phytogeographical notes on the Brazilian Amazon. Anais Acad Brasil Ciênc 25:1–46

Ferreira RD, Leão JAD, Silva TSF, Rennó CD, Novo EMLM, Barbosa CCF (2013) Atualização e correção do delineamento de áreas alagáveis da bacia Amazônica. Anais do XVI Simpósio Brasileiro de Sensoriamento Remoto, pp 5864–5871, ISBN: 978-85-17-00065-2

Forsberg BR, Castro JGD, Cargnin-Ferreira E, Rosenqvist A (2001) The structure and function of the Negro River Ecosystem: Insights from the Jau Project, In: Cgão NL, Petry P, Prang P, Sonneschein L, Tlusty M (eds.). Conservation and Management of Ornamental Fish Resources of the Rio Negro Basin. Projeto Piaba, Amazonia, pp 125–144

Hamilton SK, Kellndorfer J, Lehner B, Tobler M (2007) Remote sensing of floodplain as a surrogate for biodiversity in a tropical river system (Madre de Dios, Peru). Geomorphol 89:23–38

Hawes JE, Peres CA, Riley LB, Hess LL (2012) Landscape-scale variation in structure and biomass of Amazonian seasonally flooded and unflooded forests. For Ecol Manag 281:163–176

Henderson F, Lewis A (2008) Radar detection of wetland ecosystems: a review. Int J Remote Sens 29:5809–5835

Hess LL, Melack JM, Filoso S, Wang Y (1995) Delineation of inundated área and vegetation along the Amazon floodplain with the SIR-C synthetic aperture radar. IEEE Trans Geosci Remote Sens 33:896–904

Hess LL, Melack JM, Novo EMLM, Barbosa CCF, Gastil M (2003) Dual-season mapping of wetland inundation and vegetation for the Central Amazon Basin. Remote Sens Environ 87:404–428

Hess LL, Affonso AG, Arraut EM, Novo EMLM, Gielow R, Renó V, Barbarisi B and Marioni B (2011) Evaluation of low-cost tree-mounted temperature loggers for validation of satellite-based flood mapping on the Amazon floodplain. Anais XV Simpósio Brasileiro de Sensoriamento Remoto, pp 5278–5283, ISBN: 978-85-17-00057-7

Hueck K (1966) Die Wälder Südamerikas. Gustav Fischer Verlag, Stuttgart, p 422

IDSM. Banco de dados fluviométrico da Reserva de Desenvolvimento Sustentável Mamirauá. http://www.mamiraua.org.br/fluviometrico. Accessed 8 Mar 2013

Irion G, Junk WJ, Mello JA (1997) The large central Amazonian river floodplains near Manaus: geological, climatological, hydrological an geomorphological aspects. In: Junk WJ (ed) Ecological studies, vol 126., The Central Amazon floodplain: ecology of a pulsating systemSpringer-Verlag, Berlin, pp 23–46

Japan Space Systems (2012) PALSAR User's Guide, 69 p. http://gds.palsar.ersdac.jspacesystems.or.jp/e/guide/pdf/U_Guide_en.pdf. Accessed 29 Oct 2013

Junk WJ (1989) Flood tolerance and tree distribution in central Amazonian floodplains. In: Holm-Nielsen LB, Nielsen IC, Balslev H (eds) Tropical forests: botanical dynamics, speciation and diversity. Academic Press, London, pp 47–64

Junk WJ (1997) The Central Amazon floodplain: ecology of a pulsing system. Ecological studies, vol 126. Springer-Verlag, Berlin

Junk WJ, Bayley PB, Sparks RE (1989) The flood pulse concept in river-floodplain-systems. Can Spec Publ Fish Aquat Sci 106:110–127

Junk WJ, Piedade MTF, Schöngart J, Cohn-Haft M, Adeney JM, Wittmann F (2011) A classification of major naturally occurring Amazonian lowland wetlands. Wetlands 31:623–640

Junk WJ, Piedade MTF, Schöngart J, Wittmann F (2012) A classification of major natural habitats of Amazonian white-water river floodplains (várzeas). Wetl Ecol Manag, 20(6):461–475. http://link.springer.com/10.1007/s11273-012-9268-0. Accessed 8 Aug 2013

Kasischke ES, Melack JM, Dobson MC (1997) The use of imaging radars for ecological applications: a review. Remote Sens Environ 596:141–156

Lesack LFW, Melack JM (1995) Flooding hydrology and mixture dynamics of lake water derived from multiple sources in an Amazon floodplain lake. Water Resour 31:329–346

Liaw A, Wierner M (2002) Classification and regression by random: forest. RNews 2(3):18–22

Lima DS, Marmontel M, Bernard E (2012) Site and refuge use by giant river otters (*Pteronura brasiliensis*) in the Western Brazilian Amazonia. J Nat Hist 46(11–12):729–739

Lindenmayer DB, Hobbs RJ, Montague-Drake R et al (2008) A checklist for ecological management of landscapes for conservation. Ecol Lett 11:78–91. doi:10.1111/j.1461-0248.2007.01114.x

Malhi Y, Betts RA, Roberts JT et al (2008) Climate change, deforestation, and the fate of the Amazon. Science 319:169–172

Martinez J, Letoan T (2007) Mapping of flood dynamics and spatial distribution of vegetation in the Amazon floodplain using multitemporal SAR data. Remote Sens Environ 108(3):209–223. http://linkinghub.elsevier.com/retrieve/pii/S0034425706004585. Accessed 9 Aug 2013

Melack JM, Coe MT (2013) Climate change and the floodplain lakes of the Amazon basin. In: Goldman CR, Kumagai M, Robarts R (eds) Climate change and inland waters: impacts and mitigation for ecosystems and societies. Wiley, New York

Melack JM, Hess LL (2010) Remote sensing of the distribution and extent of wetlands in the Amazon basin. In: Junk WJ, Piedade MTF, Wittman F, Schöngart J, Parolin P (eds) Amazonian floodplain forests: ecophysiology, biodiversity and sustainable management. Springer, Berlin/Heidelberg/New York

Melack JM, Novo EMLM, Forsberg BR, Piedade MTF, Maurice L (2009) Floodplain ecosystem processes. In: Keller M, Bustamante M, Gash J, Dias PJ (eds) Amazonia and global change, vol 186., Geophysical monographs seriesAmerican Geophysical Union, Washington DC, pp 525–541

Mertes LAK, Daniel DL, Melack JM, Nelson B, Martinelli A, Forsberg BR (1995) Spatial patterns of hydrology, geomorphology, and vegetation on the floodplain of the Amazon River in Brazil from a remote sensing perspective. Geomorphol 13:215–232

Ozesmi SL, Bauer ME (2002) Satellite remote sensing of wetlands. Wetl Ecol Manag 10:381–402

Paim FP, Sousa J Jr, Valsecchi J, Harada ML, Queiroz HL (2013) Diversity, geographic distribution and conservation of squirrel monkeys, *Saimiri* (Primates, Cebidae), in the floodplain forests of Central Amazon. Int J Primatol 34(5):1055–1076

Parolin P, Lucas C, Piedade MTF, Wittmann F (2010) Drought responses of extremely flood tolerant trees of Amazonian floodplains. Annal Bot 105(1):129–139

Peixoto JMA, Nelson B, Wittmann F (2009) Spatial and temporal dynamics of river channel migration and vegetation in central Amazonian white-water floodplains by remote-sensing techniques. Remote Sens Environ 113(10):2258–2266. http://linkinghub.elsevier.com/retrieve/pii/S003442570900193X. Accessed 1 June 2013

Pereira MJR, Marques JT, Santana J, Santos CD, Valsecchi J, Queiroz HL, Palmeirim JM (2009) Structuring of Amazonian bat assemblages: the roles of flooding patterns and floodwater nutrient load. J Anim Ecol 78(6):1163–1171

Pires JM, Koury HM (1959) Estudo de um trecho de mata de várzea próximo a Belém. Bol Téc IAN 36:3–44

Pontius RG Jr, Millones M (2011) Death to Kappa: birth of quantity disagreement and allocation disagreement for accuracy assessment. Int J Remote Sens 32(15):4407–4429

Prance GT (1979) Notes on the vegetation of Amazonia III. The terminology of Amazonian forest types subject to inundation. Brittonia 31:26–38

Queiroz HL, Peralta N, Gatay I, Becker B (2006) Reservas de Desenvolvimento Sustentável: Manejo Integrado de Recursos Naturais e Gestão Participativa. Dimensões Humanas da Biodiversidade. Vozes, Petrópolis

Ramalho EE, Macedo J, Vieira TM, Valsecchi J, Calvimontes J, Marmontel M, Queiroz HL (2009) Ciclo Hidrológico nos ambientes de várzea da Reserva de Desenvolvimento Sustentável Mamirauá- Médio Solimões, período de 1990 a 2008. Uakari 5(1):61–87

Ramsar Convention Secretariat (2013) The Ramsar convention manual: a guide to the convention on wetlands (Ramsar, Iran, 1971), 6th ed. 112 p. Available at http://www.ramsar.org/pdf/lib/manual6-2013-e.pdf

Rennó CD, Novo EMLM, Banon LC (2013) Correção geométrica da Máscara de áreas alagáveis da bacia amazônica. Anais XV Simpósio Brasileiro de Sensoriamento Remoto, pp 5507–5514, ISBN: 978-85-17-00065-2

Renó VF, Novo EMLM, Suemitsu C, Rennó CD, Silva TSF (2011) Assessment of deforestation in the lower Amazon floodplain using historical Landsat MSS/TM imagery. Remote Sens Environ 115:3446–3456

Rodrigues WA (1961) Estudo preliminar de mata de várzea alta de uma ilha do baixo Rio Negro de solo argiloso e úmido. Pub n 10 Inst Nac Pesq Amazôn, Manaus

Rosenqvist A, Forsberg BR, Pimentel T, Rauste YA, Richey JE (2002) The use of spaceborne radar data to model inundation patterns and trace gas emissions in the Central Amazon floodplain. Int J Remote Sens 23:1303–1328

Rosenqvist A, Shimada M, Ito N, Watanabe M (2007) ALOS PALSAR: a pathfinder mission for global-scale monitoring of the environment. IEEE Trans Geosci Remote Sens 45:3307–3316

Rosenqvist A, Shimada M, Lucas R et al (2010) The Kyoto & Carbon Initiative: a brief summary. IEEE J Sel Top Appl Earth Obs Remote Sens 3:551–553

Sartori LR, Imai NN, Mura JC, Novo EMLM, Silva TSF (2011) Mapping macrophyte species in the Amazon floodplain wetlands using fully polarimetric ALOS/PALSAR Data. IEEE Trans Geosci Remote Sens 49:4717–4728

Schöngart J, Junk WJ (2007) Forecasting the flood-pulse in Central Amazonia by ENSO-indices. J Hydrol 335(1):124–132

Schöngart J, Queiroz HL (2010) Timber extraction in the Central Amazonian floodplains. In: Junk WJ, Piedade MTF, Wittmann F, Schöngart J, Parolin P (eds) Central Amazonian floodplain forests: ecophysiology, biodiversity and sustainable management. Springer, Berlin/Heidelberg/New York

Schöngart J, Junk WJ, Piedade MTF, Ayres JM, Hüttermann A, Worbes M (2004) Teleconnection between tree growth in the Amazonian floodplains and the El Niño-Southern oscillation effect. Glob Change Biol 10:683–692

Shi Z, Fung KB (1994) A comparison of digital speckle filters. In: Proceedings of IGARSS 94, Aug 8–12, pp 2129–2133

Shimada M, Isoguchi O, Tadono T, Isono K (2009) PALSAR radiometric and geometric calibration. IEEE Trans Geosci Remote Sens 47(12):3915–3932

Silva TSF, Costa MPF, Melack JM, Novo EMLM (2008) Remote sensing of aquatic vegetation: theory and applications. Environ Monit Assess 140(1–3):131–45. http://www.ncbi.nlm.nih.gov/pubmed/17593532. Accessed 8 Aug 2013

Silva TSF, Costa MPF, Melack JM (2010) Spatial and temporal variability of macrophyte cover and productivity in the eastern Amazon floodplain: a remote sensing approach. Remote Sens Environ 114:1998–2010

Silva TSF, Melack JM, Novo EMLM (2013) Responses of aquatic macrophyte cover and productivity to flooding variability on the Amazon floodplain. Glob Change Biol 19:3379–3389

Silveira R, Ramalho EE, Thorbjarnarson JB, Magnusson WE (2010) Depredation by jaguars on caimans and importance of reptiles in the diet of jaguars. J Herpetol 44(3):418–424

Sioli H (1954) Beiträge zur regionalen Limnologie des Amazonasgebietes. Arch Hydrobiol 45:267–283

Sociedade Civíl Mamirauá (1996) Mamirauá: management plan (summarized version). SCM, CNPq/MCT, Brasilía

Takeuchi M (1962) The structure of the Amazonian vegetation. 6. Igapó. J Fac Sci Univ Tokyo Sect Bot 3:297–304

Viana JP, Castello L, Damasceno JMB, Amaral ESR, Estupiñan GMB, Arantes C, Blanc D (2007) Manejo comunitário do Pirarucu *Arapaima gigas* na Reserva de Desenvolvimento Sustentável Mamirauá-Amazonas, Brasil. Áreas Aquáticas Protegidas como Instrumento de Gestão Pesqueira, 4. MMA, Brasília

Walker WS, Stickler CM, Kellndorfer JM, Kirsch KM, Nepstad DC (2010) Large-area classification and mapping of forest and land cover in the Brazilian Amazon: a comparative analysis of ALOS/PALSAR and Landsat data sources. IEEE J Sel Top Appl Earth Obs Remote Sens 3(4):594–604. http://

ieeexplore.ieee.org/lpdocs/epic03/wrapper.htm?arnumber=5623307. Accessed 26 Aug 2013

Wittmann F, Anhuf D, Junk WJ (2002) Tree species distribution and community structure of central Amazonian várzea forests by remote-sensing techniques. J Trop Ecol 18:805–820

Wittmann F, Junk WJ, Piedade MT (2004) The várzea forests in Amazonia: flooding and the highly dynamic geomorphology interact with natural forest succession. For Ecol Manag 196(2–3):199–212. http://linkinghub.elsevier.com/retrieve/pii/S0378112704002439. Accessed 1 June 2013

Wittmann F, Schöngart J, Montero JC, Motzer T, Junk WJ, Piedade MTF, Queiroz HL, Worbes M (2006) Tree species composition and diversity gradients in white-water forests across the Amazon Basin. J Biogeogr 33(8):1334–1347. http://doi.wiley.com/10.1111/j.1365-2699.2006.01495.x. Accessed 29 May 2013

Wittmann F, Schöngart J, Brito JM, Oliveira-Wittmann A, Parolin P, Piedade MTF, Guillaumet JL (2010a) Manual of tree species in central Amazonian white-water floodplains: Taxonomy, Ecology, and Use. INPA, UEA, IDSM, Editora Valer, Manaus

Wittmann F, Schöngart J, Junk WJ (2010b) Phytogeography, species diversity, community structure and dynamics of central Amazonian floodplain forests. In: Junk WJ, Piedade MTF, Wittmann F, Schöngart J, Parolin P (eds) Central Amazonian floodplain forests: ecophysiology, biodiversity and sustainable management. Springer, Berlin/Heidelberg/New York